

Facile one-pot synthesis of Pt nanoparticles /SBA-15: an active and stable material for catalytic applications†

Junjiang Zhu,^{*a} Xiao Xie,^a Sónia A. C. Carabineiro,^b Pedro B. Tavares,^c José L. Figueiredo,^b Reinhard Schomäcker^a and Arne Thomas^{*a}

Received 14th January 2011, Accepted 12th March 2011

DOI: 10.1039/c1ee01040a

Pt/SBA-15 with an enhanced surface area but unchanged pore diameter (compared to pure SBA-15) and a Pt average particle size of ~9 nm shows a high and stable activity for both gas-phase CO oxidation and liquid-phase cyclooctadiene hydrogenation. No intrinsic change in the structure of the catalyst occurs after several reaction cycles, suggesting that the Pt/SBA-15 presented here is an active and stable catalyst.

Supported noble metal catalysts are widely used in industrial applications due to their excellent catalytic performances, either for high temperature gas-phase reactions (*e.g.* purification of exhaust gas)^{1–3} or for moderate temperature liquid-phase reactions (*e.g.* synthesis of organic chemicals)^{4–6} or others.^{7,8} However, as supported noble metals are prone to aggregation and leaching during reactions, deactivation often occurs quickly, which obviously should be avoided considering the high costs of these catalysts. Therefore, preparation

of noble metal catalysts with good catalytic performance, but also high stability, is essential for practical applications.

Bulk noble metals are expensive and have low surface areas thus show none or low catalytic activity. Therefore, supports are frequently used on which small nanoparticles of the noble metals are immobilized, yielding an increased number of accessible active sites and thus decreasing the cost and increasing the catalytic performance.⁹ However, for the preparation of such catalysts some issues have to be addressed, *e.g.* finding suitable preparation methods, the selection of supports, the choice of the metal precursors, *etc.*, as different materials or technologies used can lead to diverse catalytic properties.

Porous silicas are one of the most commonly used supports for noble metals. In this respect SBA-15 type silica^{10–13} has received a lot of attention since it was first reported, and, at least in the scientific literature, it is now one of the most widely used supports in catalysis. This is due to the straightforward synthesis and its highly defined textural properties, such as the high surface area, ordered pore structure, controllable pore size, *etc.* As the surface of SBA-15 is relatively inert, it is difficult to directly graft metal nanoparticles (NPs) on it. Hence, additives or surfactants are often used to functionalize the SBA-15 surface before grafting the metal NPs, and their deposition on the surface is usually carried out by a post-synthesis method.^{14–20} This often leads to formation of NPs lacking uniformity in size and shape. Furthermore, the interaction between the NPs and the support is often not strong enough, and therefore agglomeration^{20–24} or leaching^{24–29} of the catalyst during the reaction is often observed. This is true in particular for noble metal catalysts.

^aInstitut für Chemie, Technische Universität Berlin, Englische Str. 20, 10587 Berlin, Germany. E-mail: ciaczjj@gmail.com

^bLaboratory of Catalysis and Materials (LCM), Associate Laboratory (LSRE/LCM), Department of Chemical Engineering, Faculty of Engineering, University of Porto, Rua Dr Roberto Frias, 4200-465 Porto, Portugal

^cCentro de Química, Universidade de Trás-os-Montes e Alto Douro, Apartado 1013, 5001-801 Vila Real, Portugal

† Electronic supplementary information (ESI) available: Experimental details and more characterization results. See DOI: 10.1039/c1ee01040a

Broader context

Supported noble metals are active catalysts for various reactions in heterogeneous catalysis. However, there are also several problems in practical applications, such as aggregation and leaching. Preparation of highly active and stable nano-scale noble metals is an important goal of catalysis and materials scientists, as an efficient catalyst can not only reduce cost but also save energy of chemical processes. In developing the supported metal catalysts, one problem, however, is always unavoidable: the surface area and the pore size of the support decrease obviously after metal loading. This leads to a negative effect on catalytic reactions, where the surface area or the pore size plays an important role. Here, we report a new method for the preparation of a SBA-15 supported platinum catalyst, Pt/SBA-15, which shows an enhanced surface area and unchanged pore diameter comparing to pure SBA-15, and a Pt average particle size of 9.3 nm. Catalysis studies indicate that this catalyst can show a high and stable activity for both gas-phase CO oxidation and liquid-phase cyclooctadiene hydrogenation, and no intrinsic change in the structure of the catalyst occurs after several reaction cycles, suggesting that the Pt/SBA-15 presented here is a promising material for environmental catalysis use.

Recently, some efforts were made for *in situ* incorporation of noble metal NPs into the SBA-15 structure:^{30–33} Richards *et al.*³⁰ succeeded to confine Au NPs on the pore walls of SBA-15 by adding HAuCl₄ solution directly to the synthesis process. However, the sample obtained showed irregular shapes and pores; Somorjai *et al.*³² reported that Pt with particle size ranging from 1.7 nm to 7.0 nm can be deposited on SBA-15 in the presence of poly(vinylpyrrolidone) (PVP), but the surface area and/or the pore size of the samples significantly decreased when compared to the pure SBA-15.

In a recent work, we have shown that the introduction of poly(vinylalcohol) (PVA) to the synthesis process of SBA-15 can create additional mesopore connectivities in the structure, leading to an overall increased surface area and pore volume, while keeping the mesopore size and structure unchanged.³⁴ Using the same strategy, the introduction of PVA stabilized Pt nanoparticles to SBA-15 during synthesis was tested in this work. It was found that the obtained SBA-15 material with incorporated Pt NPs, Pt/SBA-15, also show an increased surface area and unchanged mesopore size when compared to the parent SBA-15. This is essentially different from other Pt loaded porous silicas,^{32,33,35–37} which in general showed a decrease of surface area of SBA-15 after addition of Pt, regardless of the used additional agent. Moreover, catalytic tests indicated that the Pt/SBA-15 material prepared by the method presented here shows a high and stable activity either for gas-phase CO oxidation or for liquid-phase cyclooctadiene hydrogenation, suggesting that this material has great potential for practical applications.

The catalyst was synthesized using a similar procedure as reported for SBA-15,^{10–13} except that addition of a PVA stabilized Pt sol was included. The obtained catalysts were named based on the initial weight percent of Pt in SBA-15, for example, 0.5% Pt/SBA-15 means that the weight ratio of Pt (calculated from H₂PtCl₆) to SiO₂ (calculated from tetraethoxysilane (TEOS)) is 0.005 to 0.995. The Pt loading was confirmed by Inductively Coupled Plasma (ICP) measurements and is shown in Table S1†.

Fig. 1 shows the results obtained from X-Ray Diffraction (XRD) measurements at small angles, showing that all samples exhibit an intense peak at $2\theta = 0.8\text{--}0.9$ that corresponds to the (100) diffraction of the SBA-15 2D-hexagonal structure, indicating that its ordered pore structure remains unchanged after Pt addition. The well-resolved (110) and (200) diffraction peaks also indicate that there is no substantial change in the pore structure of samples after Pt

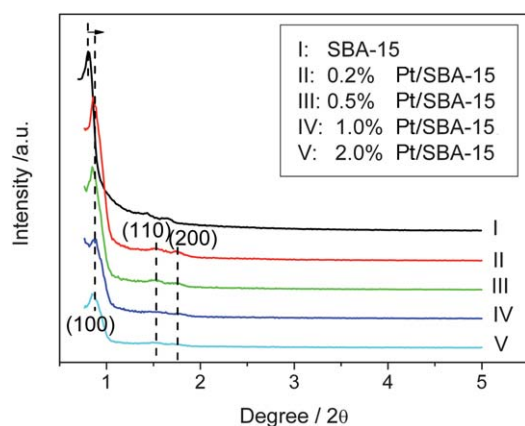


Fig. 1 XRD patterns of pure SBA-15 and that after incorporation of several amounts of Pt.

addition. A slight shift of the (100) peak position after Pt incorporation to higher angles indicates a small decrease of the unit cell.

N₂ sorption isotherms are depicted in Fig. 2 and show that all materials exhibit a well defined step with a hysteresis loop corresponding to the filling of mesopores with narrow pore size distributions, confirming that the addition of Pt does not change the mesoporous structure of SBA-15, as already indicated by XRD. Interestingly, it was found that the pore size distribution of SBA-15, with or without the addition of Pt, remains unchanged, with a value of ~ 9.5 nm. On the other hand, the surface area of SBA-15 increased significantly after the addition of Pt, from 877 m² g⁻¹ for the pure SBA-15 to, for example, 1300 m² g⁻¹ for 0.5 wt% Pt/SBA-15 (the other porosity values can be found in Table S1†; calculations were made as described in the literature³⁸). The increased surface area is due to the additional mesopore connectivities created by PVA, which therefore seems to have the ability to prevent aggregation of Pt NPs as well as to create new pores in the SBA-15 structure. Indeed, the surface area of SBA-15–PVA sample (with no Pt addition) also increased in comparison to that of pure SBA-15. Nevertheless, it should be pointed out that the surface area and pore volume of SBA-15 also increased after Pt incorporation. To the best of our knowledge, this is the first report showing that noble metal incorporation on SBA-15 can be accompanied with an increase in surface area, while keeping the mesopore size unchanged at the same time. Although in several previous works it was shown that addition of supplementary agents can increase the surface area of SBA-15, no report exists on the simultaneous improvement of the surface area, after the incorporation of metal NPs, independently of the supplementary agent. This method also works for other metals such as gold (*i.e.* Au/SBA-15, see Fig. S2†). These unexpected properties suggest that the current

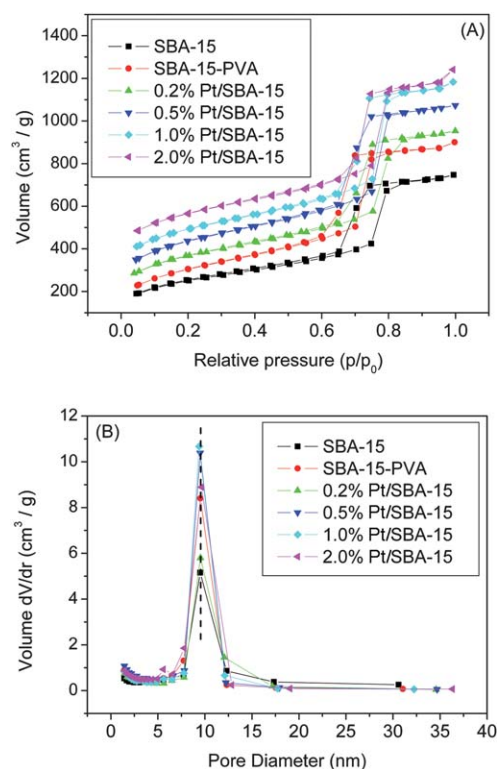


Fig. 2 N₂ sorption isotherms (A) and pore size distributions (B) of pure SBA-15 and after addition of PVA and various Pt contents.

Pt/SBA-15 material would exhibit additional interesting performances in practical use, where the influence of the surface area or the pore size of the catalyst needs to be considered.

Transmission Electron Microscopy (TEM) images were obtained in order to check the ordered structure of Pt/SBA-15 and to measure the particle size of Pt NPs. The results presented in Fig. 3 show that the 0.5% Pt/SBA-15 samples have a 2D hexagonal structure as that of pure SBA-15, confirming that the addition of PVA or Pt did not change the ordered structure of SBA-15. An overview image (Fig. 3(A)) shows that the Pt particles were highly dispersed in the SBA-15 structure and that the Pt particle size varies between 4.1 nm and 15.5 nm (average *ca.* 9.3 nm, Fig. 3(B)), and does not change much with the Pt loading (TEM images of the other samples can be found in Fig. S3†), suggesting that this method is favorable for preparing a highly dispersed Pt/SBA-15 material. Although it cannot be excluded that Pt NPs are located on the outer surface of SBA-15, careful observation indicates that at least some of the Pt NPs are incorporated into the pores of SBA-15 (Fig. 3(C)).

Fig. 4(A) shows the catalytic activities of the Pt/SBA-15 materials for gas-phase CO oxidation reaction. Although no substantial change in the activity of pure SBA-15 and 0.2% Pt/SBA-15 was observed, a significant decrease in the temperature for complete conversion of CO was observed with 0.5% Pt/SBA-15, from 400 °C for pure SBA-15 to 300 °C for 0.5, 1.0 and 2.0% Pt/SBA-15, indicating that Pt incorporation can decrease the temperature of total CO conversion. The ignition temperature (~ 300 °C) of the Pt/SBA-15 for CO oxidation observed here is in agreement with that of Pt/mSiO₂ reported by Somorjai *et al.*³⁹ This temperature lies between that of Pt(100) (227 °C) and Pt(111) (347 °C) single crystals, thus suggesting that the Pt NPs on SBA-15 are mostly composed by cubic and cuboctahedron shapes, which expose mostly the (100) and (111) surfaces³⁹ (see the HRTEM image in Fig. 3(D)). The jump in the ignition temperature from 0.2% Pt/SBA-15 to 0.5% Pt/SBA-15 implies that there is a threshold Pt loading for CO oxidation reaction,

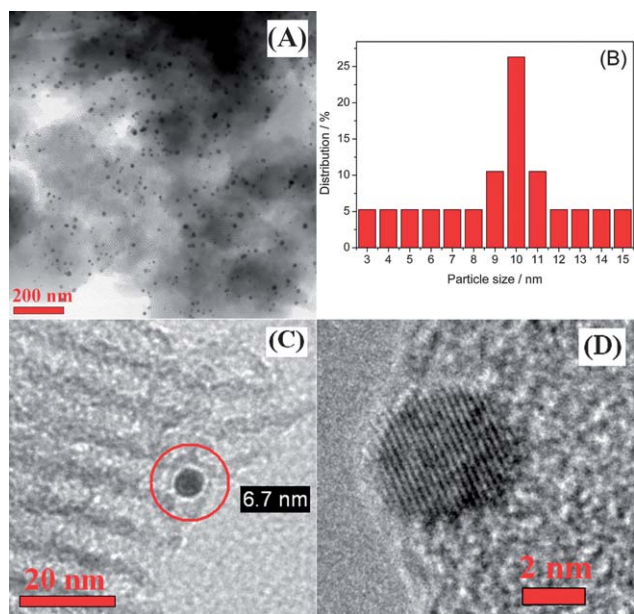


Fig. 3 TEM images of 0.5% Pt/SBA-15. (A) Overview image; (B) particle size distribution of Pt NPs; (C) image showing small particles are in the pore of SBA-15; (D) high resolution TEM image.

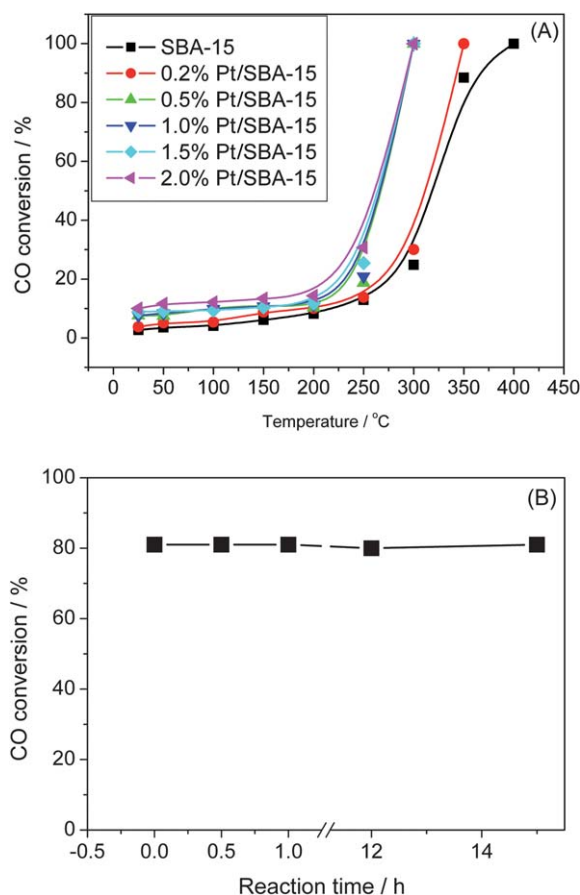


Fig. 4 (A) CO conversion of SBA-15 with or without the incorporation of Pt at different temperatures; (B) long-time stability test for 0.5% Pt/SBA-15 in CO oxidation at 290 °C.

below which value the catalyst cannot work efficiently. However, no significant increase in the activity was observed above this value (*i.e.* from 0.5% to 2.0% Pt/SBA-15), indicating that the Pt loading in 0.5% Pt/SBA-15 is enough. Long-time activity tests in Fig. 4(B) show that the CO oxidation activity ($\sim 81\%$ CO conversion) of sample 0.5% Pt/SBA-15 remains unchanged, even after being carried out at 290 °C for 15 hours, indicating a very stable activity for the reaction.

For comparison, an additional catalyst prepared by the post-synthesis method (1 wt% Pt/SBA-15—post) was also tested, but it was found that Pt was not easily loaded on the SBA-15 and, therefore, its activity was similar to that of pure SBA-15.

Based on the results shown in CO oxidation, sample 0.5% Pt/SBA-15 was chosen as a test catalyst for liquid phase reaction and the results are shown in Fig. 5, where cyclooctadiene (COD) hydrogenation was used as a model reaction. The COD conversion reached $\sim 90\%$ within 35 min at 70 °C, indicating that the catalyst is very active for this reaction. The change of the activity with time was not monitored due to the short reaction time, and thus only the final activity was measured. The reusability of the catalyst was tested by first removing the used reactant, and then washing the catalyst with heptane 3 times (the removal of the used reactant and the washed heptane was done with the help of a pump), after that the reactor was refilled with fresh COD and the new reaction started. The obtained results can be found in Fig. 5, which shows that the catalyst can work up to 6 runs (the maximum tested) with no appreciable loss in the

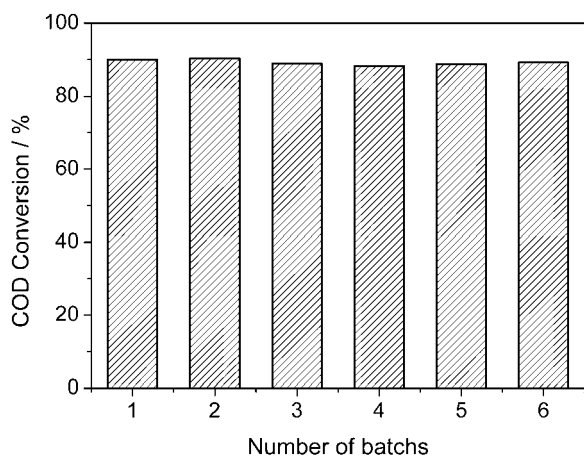


Fig. 5 Activity and reusability of 0.5% Pt/SBA-15 for cyclooctadiene hydrogenation; *reaction conditions*: 1 g catalyst + 1.13 mL cyclooctadiene + 60 mL heptane (solvent), 70 °C, $P_{H_2} = 1.1$ bar. (Weight loss of the catalyst during the pumping process was taken into consideration when calculating the activity at each batch.)

activity, suggesting that the Pt/SBA-15 sample is stable and has good reusability for liquid phase reaction.

Hence, it can be concluded that the current Pt/SBA-15 material is active and can show stable activity either for gas-phase CO oxidation or for liquid-phase COD hydrogenation, satisfying the requirements of a catalyst for industrial application. To check if any changes occurred in the catalyst after usage, studies on the catalyst after reaction were carried out, and the results are shown in Fig. 6. N_2 sorption isotherms and pore size distributions (Fig. 6(A)) show that there is no intrinsic change in the catalyst before and after CO oxidation, and the minor difference found in the surface area is within the experimental error (<5%). However, a slight decrease in the surface area and pore size was detected after the hydrogenation reaction, which could be due to: (1) coke accumulation on the pore wall of the catalyst and (2) shrinkage of the material during the reaction. Indeed, the XRD measurements shown in Fig. 6(B) show a small shift in the (100) peak position to higher angles after COD hydrogenation (curve “U2”). However, TGA tests show that there was no appreciable difference in the weight loss of the catalyst before and after the reaction (see Fig. S6†). Hence, it can be inferred that the decrease in the surface area and pore size after 6 runs in COD hydrogenation reaction is due to the shrinkage of the porous structure of the sample. Still, the unchanged COD conversion after those runs suggests that this shrinkage does not significantly influence the catalytic performances. TEM images of the catalyst after CO oxidation and COD hydrogenation reaction are shown in Fig. 6(C) and (D), respectively, showing that the well ordered structure of the materials is maintained during the reactions. Furthermore, no intrinsic change in the particle size before and after the reaction was observed, suggesting that the Pt NPs are very stable and that no aggregation occurs during the reaction, even for the gas phase CO oxidation performed at 300 °C. Metal leaching is another factor which is often observed to lead to catalyst deactivation. Therefore the Pt loading after the COD reaction was also analyzed, and no appreciable loss was detected (see Table S1†), suggesting that Pt was well stabilized to the SBA-15 surface. As a result, it can be concluded that the here reported Pt/SBA-15 material is not only active but also highly stable for catalysis (as no aggregation at high temperatures and no leaching in liquid phase reaction occurred).

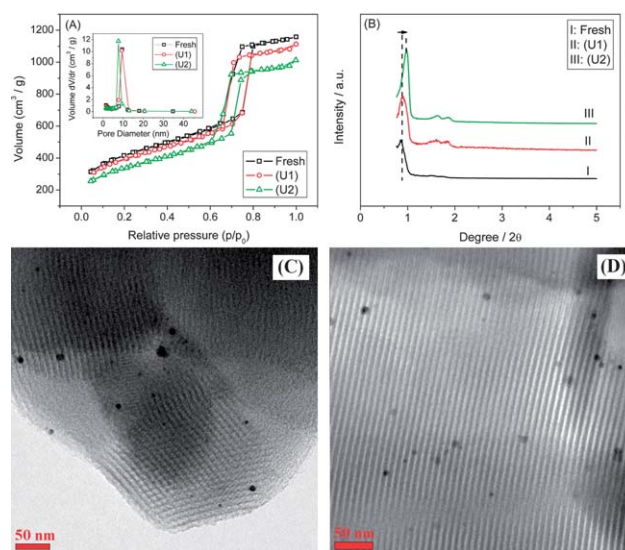


Fig. 6 Characterizations of 0.5% Pt/SBA-15 sample after reaction; (A) N_2 sorption isotherms and the corresponding pore size distributions (inset); (B) XRD patterns at small angles (Note: “U1” is the used catalyst after CO oxidation and “U2” is the used catalyst after cyclooctadiene hydrogenation); (C) TEM images of U1; (D) TEM images of U2.

The high stability of the Pt/SBA-15 catalyst might come from its efficient synthesis method. That is, the Pt NPs were first prepared and protected by PVA, and then *in situ* incorporated into the SBA-15 structure. This way the Pt NPs are highly dispersed and well embedded in the SBA-15 structure, avoiding aggregation and/or leaching during the reaction.

In summary, we showed in this work that platinum nanoparticles can be simply incorporated into the SBA-15 structure by a facile one-pot synthesis method. Unlike what was reported in previous works, the results shown here indicate that the surface area of SBA-15 can increase significantly after Pt incorporation, while the mesopore size is kept unchanged. This is due to the presence of PVA in the Pt sol. Catalytic tests indicate that the prepared Pt/SBA-15 material is active either for gas-phase CO oxidation or for liquid-phase cyclooctadiene hydrogenation. Furthermore, the material is highly stable in the reaction and no appreciable loss in the activity was observed in the long-term activity tests, suggesting that the present Pt/SBA-15 is a highly active and stable material for catalytic uses, satisfying the requirements of a catalyst for industrial application.

Acknowledgements

Dr Yilmaz Aksu from the Technical University of Berlin is acknowledged for the measurement of TGA curves. Financial support from the German Research Foundation (DFG, grant No. TH 1463/5-1) and the Cluster of Excellence “Unifying Concepts in Catalysis” (EXL 31411) is gratefully acknowledged.

References

- W. Tang, Z. P. Hu, M. J. Wang, G. D. Stucky, H. Metiu and E. W. McFarland, *J. Catal.*, 2010, **273**, 125–137.
- A. C. Gluhoi, N. Bogdanchikova and B. E. Nieuwenhuys, *Catal. Today*, 2006, **113**, 178–181.
- F. Tao, S. Dag, L. W. Wang, Z. Liu, D. R. Butcher, H. Bluhm, M. Salmeron and G. A. Somorjai, *Science*, 2010, **327**, 850–853.

- 4 J. J. Zhu, S. A. C. Carabineiro, D. Shan, J. L. Faria, Y. J. Zhu and J. L. Figueiredo, *J. Catal.*, 2010, **274**, 207–214.
- 5 C. E. Chan-Thaw, A. Villa, P. Katekomol, D. S. Su, A. Thomas and L. Prati, *Nano Lett.*, 2010, **10**, 537–541.
- 6 D. Wang, F. Ammari, R. Touroude, D. S. Su and R. Schlögl, *Catal. Today*, 2009, **147**, 224–230.
- 7 J. S. chen, C. P. Chen, J. Liu, R. Xu, S. Z. Qiao and X. W. Lou, *Chem. Commun.*, 2011, **47**, 2631–2633.
- 8 J. Liu, S. Z. Qiao, S. B. Hartono and G. Q. Lu, *Angew. Chem., Int. Ed.*, 2010, **49**, 4981–4985.
- 9 J. J. Zhu, Y. C. Wei, W. K. Chen, Z. Zhao and A. Thomas, *Chem. Commun.*, 2010, **46**, 6965–6967.
- 10 D. Y. Zhao, J. L. Feng, Q. S. Huo, N. Melosh, G. H. Fredrickson, B. F. Chmelka and G. D. Stucky, *Science*, 1998, **279**, 548–552.
- 11 D. Y. Zhao, Q. S. Huo, J. L. Feng, B. F. Chmelka and G. D. Stucky, *J. Am. Chem. Soc.*, 1998, **120**, 6024–6036.
- 12 D. Y. Zhao, J. Y. Sun, Q. Z. Li and G. D. Stucky, *Chem. Mater.*, 2000, **12**, 275.
- 13 A. Galarneau, N. Cambon, F. Di Renzo, R. Ryoo, M. Choi and F. Fajula, *New J. Chem.*, 2003, **27**, 73–79.
- 14 Z. J. Wang, Y. B. Xie and C. J. Liu, *J. Phys. Chem. C*, 2008, **112**, 19818–19824.
- 15 Z. L. Zheng, H. F. Li, T. F. Liu and R. Cao, *J. Catal.*, 2010, **270**, 268–274.
- 16 W. Huang, J. N. Kuhn, C. K. Tsung, Y. Zhang, S. E. Habas, P. Yang and G. A. Somorjai, *Nano Lett.*, 2008, **8**, 2027–2034.
- 17 B. Lee, Z. Ma, Z. T. Zhang, C. Park and S. Dai, *Microporous Mesoporous Mater.*, 2009, **122**, 160–167.
- 18 X. Y. Liu, A. Q. Wang, X. D. Wang, C. Y. Mou and T. Zhang, *Chem. Commun.*, 2008, 3187–3189.
- 19 C. Y. Ma, B. J. Dou, J. J. Li, J. Cheng, Q. Hu, Z. P. Hao and S. Z. Qiao, *Appl. Catal., B*, 2009, **92**, 202–208.
- 20 Y. S. Cho, J. C. Park, B. Lee, Y. Kim and J. H. Yi, *Catal. Lett.*, 2002, **81**, 89–96.
- 21 M. N. Timofeeva, S. H. Jhung, Y. K. Hwang, D. K. Kim, V. N. Panchenko, M. S. MeGunov, Y. A. Chesalov and J. S. Chang, *Appl. Catal., A*, 2007, **317**, 1–10.
- 22 C. P. Huang and Y. H. Huang, *Appl. Catal., A*, 2008, **346**, 140–148.
- 23 P. Han, H. M. Zhang, X. P. Qiu, X. L. Ji and L. X. Gao, *J. Mol. Catal. A: Chem.*, 2008, **295**, 57–67.
- 24 M. N. Timofeeva, O. A. Kholdeeva, S. H. Jhung and J. S. Chang, *Appl. Catal., A*, 2008, **345**, 195–200.
- 25 D. P. Serrano, J. Aguado and C. Vargas, *Appl. Catal., A*, 2008, **335**, 172–179.
- 26 J. Demel, J. Cejka and P. Stepnicka, *J. Mol. Catal. A: Chem.*, 2010, **329**, 13–20.
- 27 P. Y. Wang, Q. S. Lu and J. G. Li, *Mater. Res. Bull.*, 2010, **45**, 129–134.
- 28 F. B. Su, L. Lv, F. Y. Lee, T. Liu, A. I. Cooper and X. S. Zhao, *J. Am. Chem. Soc.*, 2007, **129**, 14213–14223.
- 29 H. Essa, E. Magner, J. Cooney and B. K. Hodnett, *J. Mol. Catal. B: Enzym.*, 2007, **49**, 61–68.
- 30 J. C. Hu, L. F. Chen, K. K. Zhu, A. Suchopar and R. Richards, *Catal. Today*, 2007, **122**, 277–283.
- 31 D. Tian, G. P. Yong, Y. Dai, X. Y. Yan and S. M. Liu, *Catal. Lett.*, 2009, **130**, 211–216.
- 32 H. Song, R. M. Rioux, J. D. Hoefelmeyer, R. Komor, K. Niesz, M. Grass, P. D. Yang and G. A. Somorjai, *J. Am. Chem. Soc.*, 2006, **128**, 3027–3037.
- 33 R. M. Rioux, R. Komor, H. Song, J. D. Hoefelmeyer, M. Grass, K. Niesz, P. D. Yang and G. A. Somorjai, *J. Catal.*, 2008, **254**, 1–11.
- 34 J. J. Zhu, K. Kailasam, X. Xie, R. Schomaecker and A. Thomas, *Chem. Mater.*, 2011, DOI: 10.1021/cm1028639.
- 35 C. M. Yang, P. H. Liu, Y. F. Ho, C. Y. Chiu and K. J. Chao, *Chem. Mater.*, 2003, **15**, 275–280.
- 36 Z. Konya, E. Molnar, G. Tasi, K. Niesz, G. A. Somorjai and I. Kiricsi, *Catal. Lett.*, 2007, **113**, 19–28.
- 37 J. Liu, Q. Yang, X. S. Zhao and L. Zhang, *Microporous Mesoporous Mater.*, 2007, **106**, 62–67.
- 38 J. Liu, Q. H. Yang, L. Zhang, H. Q. Yang, J. S. Gao and C. Li, *Chem. Mater.*, 2008, **20**, 4268–4275.
- 39 S. H. Joo, J. Y. Park, C. K. Tsung, Y. Yamada, P. D. Yang and G. A. Somorjai, *Nat. Mater.*, 2009, **8**, 126–131.